Benefits of 3D Collagen Gels

Embedding cells within a collagen matrix was the cell culturing technique chosen to design the bioreactor described in the manuscript around. By providing a component of the native microenvironment with collagen fibers and by having a 3D architecture with high confluence, the environment is more similar to *in vivo* than many other cell culturing techniques. To illustrate different cell culturing techniques and their similarity to in vivo conditions, we created the schematic shown in **Supporting Information Figure S1**.

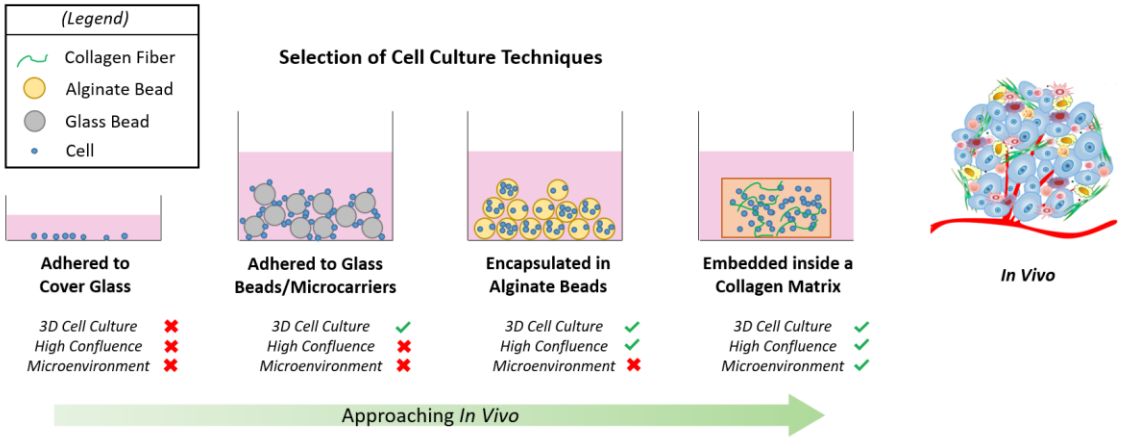

Supporting Information Figure S1: Key differences between common cell culturing techniques. Schematics representing common cell culturing techniques are shown from left to right with increasing similarity to the in vivo environment. Key attributes that mimic in vivo conditions are listed below each method with check mark to indicate its presence for a given technique.

Diffusion Model

During magnetic resonance spectroscopy (MRS) experiments inside the bioreactor, hyperpolarized [1-^{13}C] Pyruvate is injected into the sample volume. This volume contains a collagen gel with cells suspended inside it along with a sub-volume of medium surrounding the collagen gel.

Upon dissolution, the hyperpolarization of the substrate decays back to thermal equilibrium, resulting in a loss of signal after about 2-3 minutes. The observed lactate signal depends on the ability of the substrate to diffuse into the collagen gel before that loss of signal. Therefore, an estimate of the diffusion of pyruvate into the collagen gel over the time course of an MRS experiment would help explain observed signals and elucidate the mechanics of delivering a substrate to the embedded within the gel.

Diffusion Model

There are many models of diffusion and they are outlined at length in *The Mathematics of Diffusion* by John Crank [1]. Most situations can be adequately described by applying Fick's Laws of Diffusion.

In particular, it is possible to derive a concentration profile at a boundary between two reservoirs with different concentrations, by solving Fick's Second Law of Diffusion with the appropriate initial conditions [1]:

$$\frac{\partial C}{\partial t} = D\frac{\partial^2 C}{\partial x^2} \qquad (1)$$

This form of Fick's Second Law assumes that the diffusion coefficient for the molecule and medium in question is constant in all directions, which is appropriate for most situations. A closer examination of the situation of the collagen gel in medium immediately following injection of hyperpolarized pyruvate allows for the selection of initial conditions to build an appropriate diffusion model.

Supporting Information S2A depicts a simplified schematic of a pyruvate injection inside the sample volume of the bioreactor. Immediately following a pyruvate injection, there is a bolus of pyruvate at the top of the sample volume, which can then spread out throughout the media, before diffusing into the collagen gel.

This is clearly a simplification of the problem, as some pyruvate will diffuse into the gel as it spreads out through the sample volume, and the diffusion throughout the medium and into the gel are not discrete steps. However, for the purposes of this model, and to derive an estimate of the diffusion into the gel, it will be assumed that the pyruvate spreads through the medium quickly and then into the gel through a slower diffusion step.

Using this assumption, we have the much more straightforward case of an initial uniform concentration of pyruvate in the medium with a zero concentration inside the gel at t ~ 0, as shown in **Supporting Information Figure S2B**.

This simplified case allows us to solve Fick's Second Law (above) with the following initial conditions:

$C = C_o$ for $x < 0$ (outside the gel) and $C = 0$ for $x > 0$ (inside the gel) at $t = 0$.

This yields the following equation for pyruvate concentration as a function of position relative to the gel (x) and time (t) [1]:

$$C(x,t) = \frac{1}{2}C_o erfc\frac{x}{2\sqrt{Dt}} \qquad (2)$$

The above equation can be solved for different times after t = 0 to get a sense of the concentration profile of pyruvate at the edge of the gel.

However, the above equation also depends on D, the diffusion coefficient for the hyperpolarized pyruvate in a collagen gel.

Diffusion Coefficient of Pyruvate

Diffusion coefficients vary with the particle diffusing, the medium through which it diffuses and the temperature of the medium. Therefore, finding specific diffusion coefficients for a particular setup can be difficult. Usually, for unique cases, these are measured by watching dyes diffuse into a given medium.

Sogaard et al. made a measurement of the diffusion coefficients of hyperpolarized ^{13}C-labeled metabolites, using diffusion weighting combined with hyperpolarized MRS [2]. Their work included ^{13}C-Pyruvate and was measured *in vivo*, providing a reasonable value to use for this estimate.

Averaging all of Sogaard et al.'s measurements for the diffusion coefficient of ^{13}C-Pyruvate *in vivo* yields [2]:

$$D = 1.266\ \mu m^2/ms \qquad (3)$$

Diffusion Model Results

Supporting Information Figure S2C shows three concentration profiles at the edge of the gel using the diffusion coefficient for pyruvate from Equation 3 to solve Equation 2 for the cases of t = 60 seconds, 120 seconds and 180 seconds.

This estimation of the diffusion of pyruvate into the bioreactor predicts that small amounts of pyruvate will reach 1.5 mm into the gel by t = 3 minutes. Furthermore, the depth at which there is 10% of the initial concentration of pyruvate is 0.5 mm, 0.75 mm and 0.8 mm for t = 1, 2 and 3 minutes, respectively.

Sources

1. Crank J. The Mathematics of Diffusion. 2 edition. Oxford: Oxford University Press; 1980.
2. Søgaard LV, Schilling F, Janich MA, Menzel MI, Ardenkjaer-Larsen JH. In vivo measurement of apparent diffusion coefficients of hyperpolarized ^{13}C-labeled metabolites. NMR Biomed. 2014;27: 561–569. doi:10.1002/nbm.3093

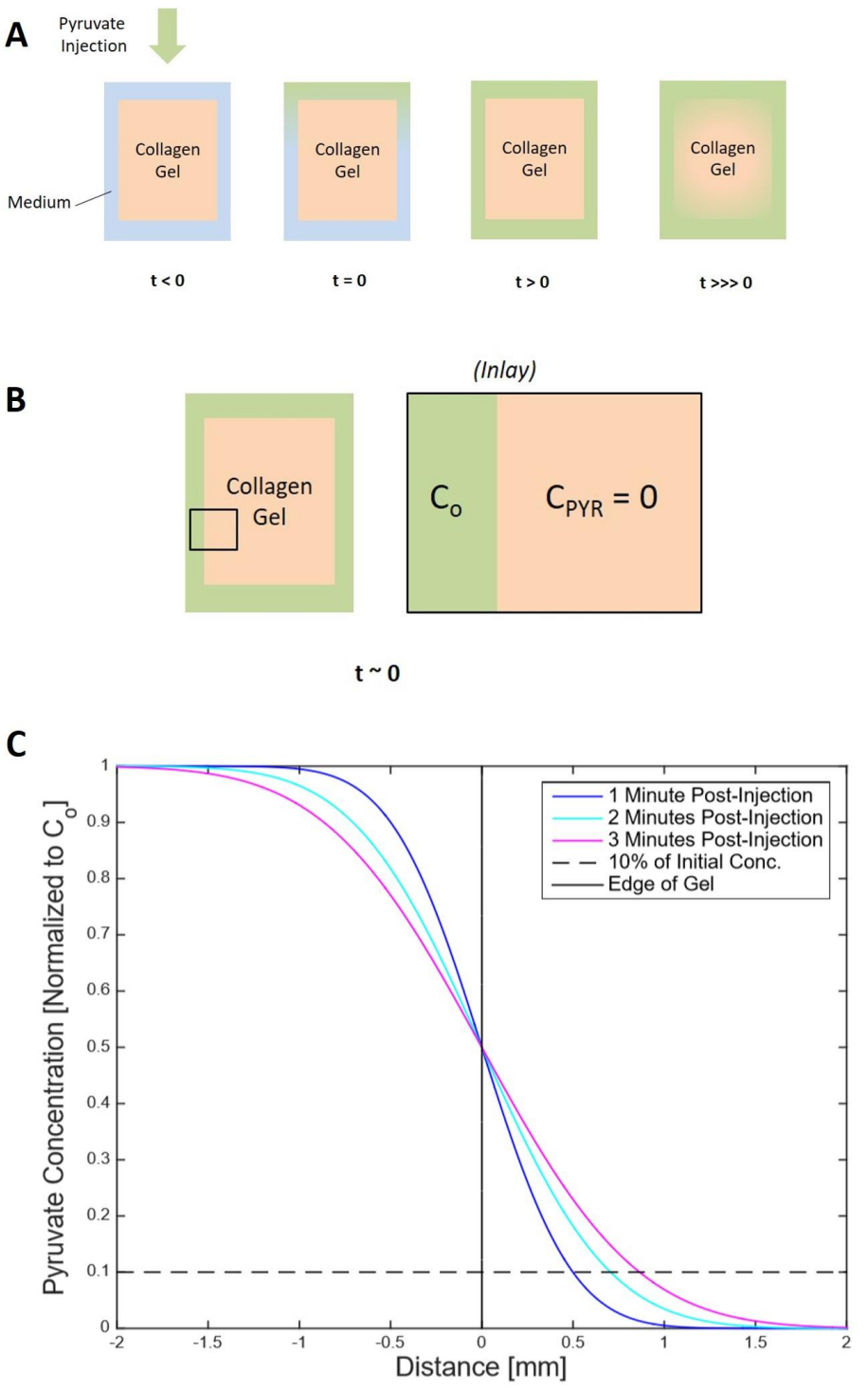

Supporting Information Figure S2: (A) Schematic of the collagen gel leading up to and after a pyruvate injection. Immediately following injection, there is a bolus of pyruvate at the top of the sample volume. The pyruvate then diffuses through the medium and then into the gel. (B) Simplified case considered in this diffusion model, with an initial concentration in the medium and a zero concentration within the gel at t ~ 0. (C) Pyruvate concentration profiles at the edge of the gel (solid black line) for t = 1, 2 and 3 minutes post injection. The 10% line (dashed black line) can be used to estimate the depth at which there is 10% of the initial pyruvate concentration at any given time point.

3D Stack Visualization of cells in collagen matrix in the Bioreactor

It can be challenging to visualize 3D images and demonstrate the range of signals for a given sample volume. This is particularly challenging in a print form. An orthogonal view of a z-stack of images is a great way to understand this. **Supporting Information Figure S3** shows an orthogonal view of a z-stack as an inlay to Panel C from Figure 1 in the manuscript. This was taken of 4T1 cells within a collagen matrix and the images shown are of NADH intensity to show the cells in the collagen gel. FIJI was used to create this view from the multiphoton collected data.

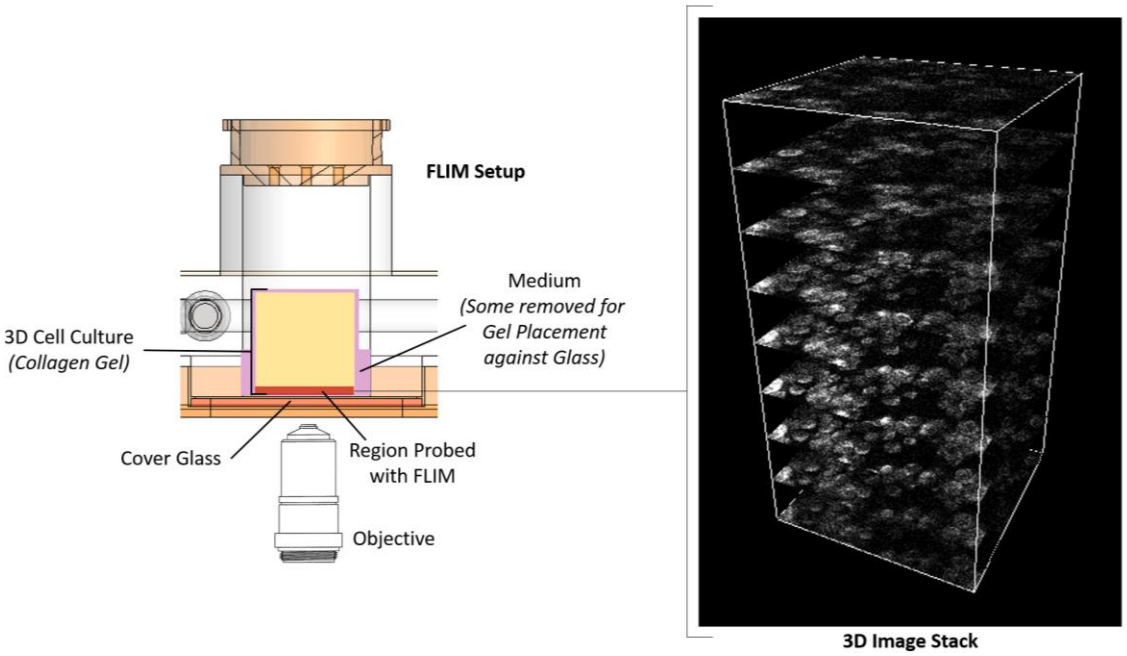

Supporting Information Figure S3: The 3D nature of optical sectioning. Cutaway view of the sample area for the FLIM experiments (left). Medium was removed and reserved to ensure that the gel contacted the cover glass for imaging. The region of the collagen gel that can be probed by optical imaging is shown in red. An orthogonal view of a z-stack of images taken through a collagen gel (inlay, right). Each image was a taken at a different depth into the sample. The signal is from NADH intensity to show the cells residing inside the collagen gel.

Cytotoxicity Study

A cytotoxicity study was performed to assess the suitability of a variety of potential materials (**Supporting Information S4**).

Cytotoxicity Study Methods

Materials for testing were in semi-circular wafers (radius = 13mm, thickness = 1.5875mm) that occupied approximately half of a well of a 6-well plate (Falcon) were generated in the follow ways:

- Polystyrene (tissue culture dish): Polystyrene wafers were cut out of existing well plates to match the material used for cell culture experiments on a Haas Mini Mill CNC Machine (Haas Automation, Oxnard, CA, USA).
- Polypropylene: Polypropylene wafers were machined out of 1/16" sheets of polypropylene (McMaster-Carr, Elmhurst, IL, USA) on a Haas Mini Mill CNC Machine (Haas Automation, Oxnard, CA, USA).
- Silicone rubber: Silicone rubber test wafers were laser cut out of 1/16" sheets of silicone rubber (McMaster-Carr, Elmhurst, IL, USA) on a PLS 6.75 laser cutter (Universal Laser Systems, Scottsdale, AZ, USA).
- Delrin: Delrin is an acetal homopolymer (DuPont). Delrin wafers were machined out of 1/16" sheets of polypropylene (McMaster-Carr, Elmhurst, IL, USA) on a Haas Mini Mill CNC Machine (Haas Automation, Oxnard, CA, USA).
- RC31: RC31 wafers were printed out of RC31 (EnvisionTEC, Dearborn, MI, USA) by LightBeam3D (Douglas, MA, USA).

MDA-231, a metastatic breast cancer cell line [35] were cultured in DMEM low glucose (Gibco, ThermoFisher Scientific) with 10% FBS (Gibco) and penicillin/streptomycin (Hyclone Laboratories Inc). Material wafers were placed into wells of a 6 well plate, one wafer per well, with one well with no material to serve as cell culture control. The wafers in the 6 well plate were UV sterilized in a biological safety cabined for 30 min, then flipped over for an additional 30 min of UV sterilization. Cells were distributed equally between the wells and allowed to attach overnight.

At 1 day, 2 day and 3 day after seeding phase microscope images of 3 regions for each well were collected. Because some of the materials were opaque, all images were taken of the area of the well without material. Note that because the materials were not attached, the materials could move, potentially dislodging some cells from the dish surface. Images were taken on a Axiovert 25 microscope (Zeiss) with a 5X Achromatic lens (NA = 0.12) for cell counts or 20X LD A Plan lens (NA = 0.5) for morphology images. Camera was an Orca R2 (Hamamatsu) and images were collected using Micromanager (Open Imaging https://micro-manager.org/). Using the cell count plug-in in FIJI (https://imagej.nih.gov/ij/plugins/cell-counter.html), the total number of cells were manually counted for each region collected and the count was divided by the area as a representative cell count on each day for each material. To adjust for variation in cell seeding density between experiments, densities were normalized either to the corresponding day 1 count (for time course graph in C) or to the corresponding polystyrene wafer measurements. Experiment was replicated on 3 different days, with one 6 well plate per replicate. Graphs and statistics generated using Prizm (GraphPad).

Cytotoxicity Study Results

Appearance of cells in the presence of PP and SR look similar to those of the controls, either no material or PS. Morphology of cells in the presence of Delrin looks similar, though a little less dense, while many of the cells in the presence of RC31 exhibit a rounded rather than stretched out morphology, as observed in the controls, and are much less dense than the controls (**Supporting Information Figure S4A**)

Cells grown in the absence of material or in the presence of PS, PP or SR generally increase in number over the 3 days, whereas cells grown in the presence of Del or RC31 do not show such an increase (**Supporting Information Figure S4B**).

Cells grown in the presence of Del exhibited some reduction in number compared to other materials, and was excluded from this device. Cells grown in close proximity to RC31 exhibited a dramatic decrease in cell number, suggesting a level of cytotoxicity. The graph indicates that trend in cell density in the presence of some materials, such as PP and SR, was similar, or higher, than control whereas it was reduced in the presence of other materials, such as Del and RC31 (**Supporting Information Figure S4C**).

Although the ability to print complex and custom designs necessitated its use in some components of the device, no components in the bioreactor that come into direct contact with the cell culture or the cell culture medium were 3D printed.

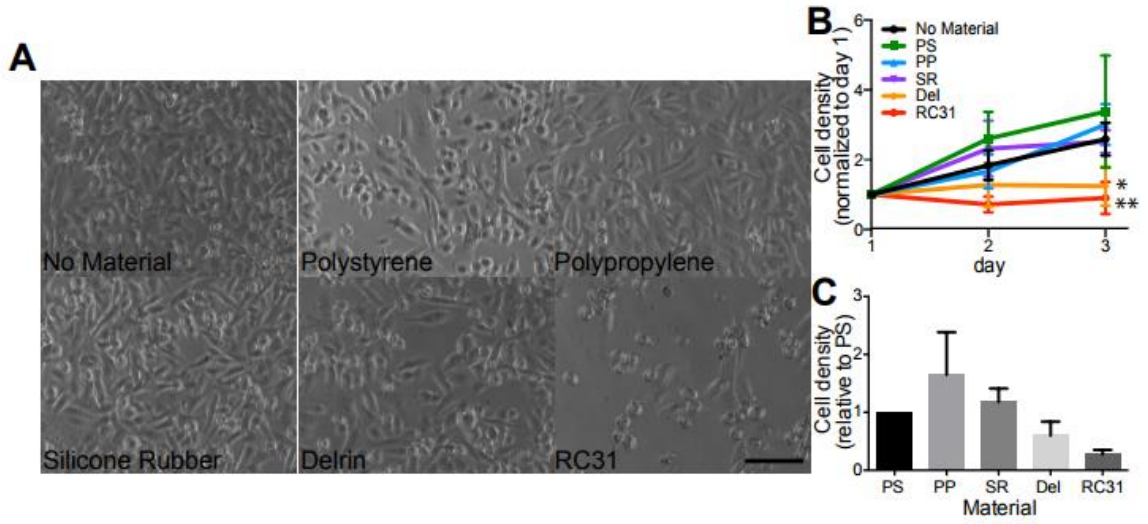

Supporting Information Figure S4: Assessment of MDA-231 cell growth on various materials. A) Brightfield images of cells grown for 3 days in wells either with no material or in the presence of materials potentially utilized for the bioreactor, including polystyrene (PS) (cell culture plastic control), polypropylene (PP), silicone rubber (SR), Delrin (del) or RC31 (RC31). (B) Graph showing the change, over 3 days, in the density of cells grown in the presence of various materials, normalized to the cell density of that treatment on day 1. ($P=0.0113$ for materials comparison, two-way ANOVA; * $P<0.05$, ** <0.01, Dunnett's multiple comparison test vs. no material control, day 3 only). C) Graph showing the cell density on day 3 relative to PS control, which takes into account mechanical disruption of cell contacts resulting from physical presence of the material wafer in the well. ($P=0.008$, one-way ANOVA; Dunnett's multiple comparisons test indicate no significant differences when compared to control PS). Scale bar is 100 microns.